The Proteomic Landscape in the Vitreous of Patients With Age-Related and Diabetic Retinal Disease

Schori, Christian ; Trachsel, Christian ; Grossmann, Jonas ; Zygoula, Ioanna ; Barthelmes, Daniel ; Grimm, Christian

Abstract: Purpose In contrast to neovascular AMD (nAMD), no treatment option exists for dry AMD. Hence, the identification of specific biomarkers is required to facilitate diagnosis and therapy of dry AMD. Methods The proteome of 34 vitreous humor samples (dry AMD: n = 6; nAMD: n = 10; proliferative diabetic retinopathy [PDR]: n = 9; epiretinal membrane [ERM]: n = 9) was analyzed by liquid chromatography coupled mass spectrometry. Then, label-free relative quantification of dry AMD, nAMD, and PDR relative to ERM, which was defined as the reference group, was performed. Application of a bioinformatics pipeline further analyzed the vitreous proteome by cluster and gene set enrichment analysis. A selection of differentially regulated proteins was validated by ELISA. Results A total of 677 proteins were identified in the vitreous of the four patient groups and quantified relatively to ERM. Different clusters of regulated proteins for each patient group were identified and showed characteristic enrichment of specific pathways including ”oxidative stress” for dry AMD, ”focal adhesion” for nAMD, and ”complement and coagulation cascade” for PDR patients. We identified cholinesterase (CHLE) to be specifically upregulated in dry AMD and ribonuclease (pancreatic; RNAS1) together with serine carboxypeptidase (probable; CPVL) to be upregulated in both forms of AMD. Conclusions The described pathways specific for the different patient groups and the identification of characteristic differentially regulated proteins provide a first step toward the definition of biomarkers for dry AMD. The presented data will facilitate the investigation of mechanistic connections of proteins to the respective disease.

DOI: https://doi.org/10.1167/iovs.18-24122

Special Issue

The Proteomic Landscape in the Vitreous of Patients With Age-Related and Diabetic Retinal Disease

Christian Schori,[1,2] Christian Trachsel,[3] Jonas Grossmann,[3] Ioanna Zygoula,[4] Daniel Barthelmes,[4,5] and Christian Grimm[1,2,6]

[1]Lab for Retinal Cell Biology, Department of Ophthalmology, University of Zurich, Zurich, Switzerland
[2]Center for Integrative Human Physiology (ZIHP), University of Zurich, Zurich, Switzerland
[3]Functional Genomics Center Zurich (FGCZ), ETH Zurich and University of Zurich, Zurich, Switzerland
[4]Department of Ophthalmology, University Hospital Zurich, Zurich, Switzerland
[5]Save Sight Institute, The University of Sydney, Sydney, Australia
[6]Neuroscience Center Zurich (ZNZ), University of Zurich, Zurich, Switzerland

Correspondence: Christian Grimm, Lab for Retinal Cell Biology, Department of Ophthalmology, University of Zurich, Wagistrasse 14, Schlieren CH 8952, Switzerland; cgrimm@opht.uzh.ch.

Submitted: February 16, 2018
Accepted: April 21, 2018

Citation: Schori C, Trachsel C, Grossmann J, Zygoula I, Barthelmes D, Grimm C. The proteomic landscape in the vitreous of patients with age-related and diabetic retinal disease. *Invest Ophthalmol Vis Sci*. 2018;59:AMD31–AMD40. https://doi.org/10.1167/iovs.18-24122

Purpose. In contrast to neovascular AMD (nAMD), no treatment option exists for dry AMD. Hence, the identification of specific biomarkers is required to facilitate diagnosis and therapy of dry AMD.

Methods. The proteome of 34 vitreous humor samples (dry AMD: $n = 6$; nAMD: $n = 10$; proliferative diabetic retinopathy [PDR]: $n = 9$; epiretinal membrane [ERM]: $n = 9$) was analyzed by liquid chromatography coupled mass spectrometry. Then, label-free relative quantification of dry AMD, nAMD, and PDR relative to ERM, which was defined as the reference group, was performed. Application of a bioinformatics pipeline further analyzed the vitreous proteome by cluster and gene set enrichment analysis. A selection of differentially regulated proteins was validated by ELISA.

Results. A total of 677 proteins were identified in the vitreous of the four patient groups and quantified relatively to ERM. Different clusters of regulated proteins for each patient group were identified and showed characteristic enrichment of specific pathways including "oxidative stress" for dry AMD, "focal adhesion" for nAMD, and "complement and coagulation cascade" for PDR patients. We identified cholinesterase (CHLE) to be specifically upregulated in dry AMD and ribonuclease (pancreatic; RNAS1) together with serine carboxypeptidase (probable; CPVL) to be upregulated in both forms of AMD.

Conclusions. The described pathways specific for the different patient groups and the identification of characteristic differentially regulated proteins provide a first step toward the definition of biomarkers for dry AMD. The presented data will facilitate the investigation of mechanistic connections of proteins to the respective disease.

Keywords: proteomics, biomarker, vitreous humor, dry AMD, nAMD

AMD is a major cause of irreversible and progressive vision loss among the elderly in the Western world.[1–3] Two patterns of retinal changes are typically distinguished and categorized as dry AMD or neovascular AMD (nAMD).[4] Dry AMD, which affects 85% to 90% of AMD patients[5,6] is characterized by the loss of RPE and subsequent atrophy of the neuroretinal tissue. nAMD is defined by the growth of new blood vessels from the choroid toward or into the retina, resulting in hemorrhages, leakage, and swelling of the neuroretinal tissue, eventually leading to subretinal scar formation.[4] Whereas in dry AMD, deterioration of vision occurs slowly, vision loss in nAMD often happens within a few months.[7–9]

Risk factors for the development of AMD include age, cigarette smoking, high body mass index, and genetic variants, mainly within the complement system.[10–15] In addition, age-dependent reduction of choroidal perfusion and resulting chronic tissue hypoxia in the retina may contribute to disease progression.[16] Research into the pathogenesis of nAMD has led to the development of drugs that target the hypoxia-induced VEGF and its signaling pathway. These drugs prevent or slow down loss of vision in the vast majority of patients with nAMD.[17–20]

For dry AMD, however, no treatment option exists. Thus, research focuses on the molecular basis of dry AMD to identify biomarkers for diagnosis and as therapeutic targets. Because direct sampling of human retina for research is difficult, alternative tissues are required as substitutes. Vitreous humor (VH) is considered a good surrogate to identify disease-specific alterations due to its close proximity to the retina, based on its at least partial reflection of the physiologic and pathologic state[21,22] and its accessibility during vitreoretinal surgery.[23–25]

Recently, mass spectrometry (MS)-based proteomics has provided a means for global proteome characterization of the human VH[26–28] and also for the analysis of ocular fluids in different eye conditions including cataract,[29] idiopathic epiretinal membranes,[30] hematogenous retinal detachment with proliferative vitreoretinopathy,[31] nAMD,[32,33] and diabetic retinopathy (DR).[23–25]

Here, we analyzed the VH proteome of eyes from patients affected by either dry AMD, nAMD, proliferative diabetic

retinopathy (PDR), or idiopathic epiretinal membranes (ERM) by liquid chromatography coupled MS (LC-MS/MS) and performed label-free relative quantification. Our results provide (1) the first report of the human VH proteome of patients affected by dry AMD; (2) a direct comparison of the dry AMD, nAMD, and PDR VH proteomes; and (3) an extended view on the major regulated pathways and characteristically regulated proteins for the different patient groups.

Methods

VH Patient Sample Collection

The study was approved by the ethics committee of Zurich, Switzerland, and adhered to the tenets of the Declaration of Helsinki. All study subjects were recruited among patients who were scheduled for elective cataract surgery or vitrectomy. Signed informed consent was obtained from each subject prior to participation. Exclusion criteria were as follows: glaucoma, intraocular surgery within the last 6 months, ocular medications other than lubricants, intraocular inflammation, nonproliferative diabetic retinopathy, myopia of more than 6 diopters spherical equivalent, any other ocular vascular disease, previous retinal detachment, previous vitrectomy, retinal degenerative disease, and presence of any other retinal condition potentially affecting either function or oxygenation of the retina other than nAMD, dry AMD, or PDR.

Of 38 patients enrolled to this single-centered study at the Department of Ophthalmology of the University Hospital Zurich, 34 (dry AMD, $n = 6$; nAMD, $n = 10$; PDR, $n = 9$; ERM, $n = 9$) were included in data analysis. Epidemiologic details of included patients are summarized in Supplementary Table S1. Four samples were excluded from further analysis for technical reasons (Supplementary Figs. S1A, S1B).

VH biopsies were collected during planned surgery, either by standard pars plana vitrectomy or the needle-tap technique[34] using a 25-gauge needle inserted 3.5 mm behind the limbus in the temporal inferior quadrant of the globe. VH samples were aspirated form the vitreous core at the start of the surgery, right after disinfection and draping. In case of cataract surgery, VH was aspirated as a first step before starting any procedure at the lens or cornea. In cases of pars plana vitrectomy, the vitreous was taken after inserting the first port in the temporal inferior quadrant before the infusion line was inserted. On average, approximately 500 µL VH were taken, independent of the used procedure. Samples were aliquoted, snap frozen, and stored in liquid nitrogen.

Sample Preparation and MS Measurement

VH samples were subjected to Agilent's Plasma 7 Multiple Affinity Removal Spin Cartridge system (MARS Hu-7; Agilent Technologies, Basel, Switzerland) for the depletion of the seven high abundant proteins (albumin, IgG, antitrypsin, IgA, transferrin, haptoglobin, and fibrinogen) according to the adapted depletion protocol by Murthy et al.[26] Depleted flow through was then pooled, desalted, and concentrated by 3-kDa nominal molecular weight limit (NMWL) low-adsorption filter membranes (Amicon Ultra-4; Merck Millipore, Schaffhausen, Switzerland). Five micrograms protein of depleted samples was subjected to filter-assisted sample preparation (FASP)-digest adapted from Wiśniewski et al.,[35] with a subsequent desalting step by C18 solid phase extraction columns (Sep-Pak Fenisterre; Waters Corp., Milford, MA, USA). Desalted tryptic peptides were lyophilized and resolubilized in 0.1% formic acid (FA). Shotgun proteomics analysis was performed on a high-resolution Fourier transformation mass spectrometer (Orbitrap Fusion; Thermo Fisher Scientific, Bremen, Germany) coupled to a nano-HPLC system (EASY-nLC 1000; Thermo Fisher Scientific). High accuracy mass spectra were acquired in the mass range of 300 to 1500 m/z and a target value of 4×10^5 ions in Orbitrap MS1, followed by top-speed MS2 via quadrupole isolation, higher energy collisional dissociation (HCD) fragmentation, and detection in the ion trap. Target ions already selected for MS2 were dynamically excluded for 25 seconds.

Protein Identification and Quantification

ProgenesisQI for proteomics software (version 3.0.5995; Nonlinear Dynamics Ltd., Tyne, UK) was used for MS1 intensity-based label-free relative quantification. The feature maps of all samples were aligned to the measurement of a representative pool of four samples per patient group. Peptides with a charge state of 2+ to 5+ were used for quantification. Top five tandem mass spectra were exported using charge deconvolution and deisotoping option at a maximum number of 200 peaks per MS2. The export was searched with Mascot database (version 2.5.1; Matrix Science, London, UK) using the following search parameters: maximum missed cleavages: 2; peptide mass tolerance: 10 ppm (# $^{13}C = 1$); and fragment ion tolerance: 0.5 Da. Carbamidomethyl on cysteine was specified as fixed, whereas oxidation on methionine and acetylation at the protein N terminus were specified as variable modifications. Searches against the human protein database (Taxonomy ID: 9606) from UniProt (59,783 entries; downloaded at 02.09.2016) concatenated to a decoy (reversed) database and 260 known MS contaminants were performed. A target-decoy approach was used to estimate the false-discovery levels.[36] Proteins with single peptide assignment and decoy hits were excluded from further analysis. For protein quantification, the normalized abundance of all nonconflicting peptide ions of the same protein group were summed together individually for each sample to generate the normalized quantitative protein abundance. Dry AMD, nAMD, and PDR patient groups were relatively quantified to the ERM patient group by pairwise comparison. Fold changes (FCs) were calculated, and statistical significance was determined by 1-way ANOVA on the hyperbolic arcsine transformed normalized protein abundance. A protein was defined to be significantly differentially regulated if it reached a $|\log_2(FC)| > 0.58$ with $P < 0.05$.

ELISA Measurement

Complement factor I (CFAI; Abnova, Walnut, CA, USA), chitinase-3-like protein 1 (CH3L1; Abnova), δ-aminolevulinic acid dehydratase (HEM2; Cloud Clone Corp., Katy, TX, USA), ribonuclease pancreatic (RNAS1; Cloud Clone Corp.), superoxide dismutase (SODC; Abnova), VEGFA (Cloud Clone Corp.), and VEGF receptor 1 (VGFR1; Cloud Clone Corp.) have been selected to be measured by sandwich-ELISA in human VH samples based on the proteomics data or their known involvement in neovascularization (VEGFA). Assays were performed according to manufacturer's instructions.

Bioinformatics

Gene ontology (GO) term enrichment and protein–protein interaction network analysis of significantly differentially regulated proteins was performed by the STRING database (version 10.5).[37] Proteins were categorized in the respective parental GO-terms "biological process" (GO-BP), "molecular function" (GO-MF), and "cellular component" (GO-CC) separately. The minimal interaction score was set to 0.3. Identification of proteases in the vitreous proteome was

performed by comparison of all significantly differentially regulated proteins to a database of all known human proteases (version 12; MEROPS DB).[38]

Volcano plots were generated by R (version 3.4.1)[39] with the RcolorBrewer (version 1.1-2 by Erich Neuwirth) package. Hierarchical Pearson clustering of $\log_2$-transformed normalized relative abundances, centered by subtraction of the average relative abundance of each protein was visualized by heatmap using the R package pheatmap (version 1.0.8 by Raivo Kolde). The area-proportional Venn diagram was generated by BioVenn.[40] Webgestalt (version 2017)[41] together with data mapping to wikipathways.org[42] was used for gene set enrichment analysis (GSEA) from gene lists ranked by $\log_2$(FC) as described by Subramanian et al.[43] The significance threshold for the enrichment was set to a false discovery rate (FDR) of 0.25.

Statistical analysis of epidemiologic and ELISA data was performed by Prism 6 software (version 6.0f; GraphPad Software, La Jolla, CA, USA). All data are presented as means ± SD. One-way ANOVA with Holm-Šídák correction for multiple comparisons was used to determine statistical significance relative to ERM group. $P < 0.05$ was considered significant.

Results

Proteomic Analysis

Of the 38 patient samples measured by LC-MS/MS, 4 samples (2 PDR and 2 ERM) were excluded for technical reasons (Supplementary Figs. S1A, S1B). The remaining 34 samples (dry AMD: $n = 6$; nAMD: $n = 10$; PDR: $n = 9$; ERM: $n = 9$) were analyzed in detail. Immunodepletion by MARS Hu-7 columns reduced the high abundant blood proteins in VH samples 10- to 500-fold (Supplementary Fig. S2).

LC-MS/MS measurements identified a total of 1,162 different proteins in the four patient groups, of which 677 were quantifiable (Supplementary Table S2) with an estimated FDR close to 0. The MS proteomics data have been deposited to the ProteomeXchange Consortium via the PRIDE[44] partner repository with the dataset identifier PXD008354.

Comparison of Patient Groups

Heatmap representation of normalized relative abundances with hierarchical clustering for proteins allowed the comparison of the different patient groups, as well as the identification of similarly regulated protein clusters (Fig. 1A). Two main clusters of upregulated proteins (shades of red) discriminated PDR (lower branch of dendrogram) from nAMD (upper branch of dendrogram) patient samples. Interestingly some patients of the dry AMD group showed similar protein regulation as patients of the nAMD group, even though they were not diagnosed with nAMD. Similarly, some nAMD samples showed a pattern comparable to the PDR group. In general, the strongest upregulation was observed for proteins in the PDR patient group.

To gain an initial overview, GO term enrichment (Fig. 1B) and protein–protein interaction network analysis (Fig. 1C; Supplementary Fig. S3) of significantly differentially regulated proteins of the patient groups was performed by STRING database. Comparison of enriched GO-BP terms identified response to stress for both dry AMD (FDR: 1.2×10^{-3}) and nAMD (FDR: 3.33×10^{-6}) and regulation of endopeptidase (FDR: 4.23×10^{-15}) for PDR as strongest enriched terms. GO-MF enriched strongly for processes related to protein binding, such as cell adhesion molecule binding for dry AMD (FDR: 1.7×10^{-3}), glycoprotein binding for nAMD (FDR: 9.0×10^{-3}), and glycosaminoglycan binding for PDR (FDR: 2.5×10^{-18}). Interestingly, extracellular region, extracellular exosome, and membrane bounded vesicle were the strongest enriched three terms for GO-CC in both forms of AMD (FDR: $< 3.7 \times 10^{-12}$). Of those, only membrane-bounded vesicle was identified among the top three in PDR (FDR: 3.4×10^{-40}). Protein–protein interaction network analysis for dry AMD identified VEGF receptor 2 (KDR), fibronectin (FN1), and intercellular adhesion molecule 1 (ICAM1) to be the network nodes with the highest degree of interaction (i.e., number of connections to other nodes) (Fig. 1C). For nAMD, this analysis identified cathepsin B (CTSB), superoxide dismutase 1 (SODC), and retinal dehydrogenase 1 (ALDH1A1) as the central nodes (Fig. 1C), whereas amyloid-β A4 protein (APP), kininogen-1 (KNG1), and metalloproteinase inhibitor 1 (TIMP1) were found to be the nodes with the highest degree for PDR (Supplementary Fig. S3). Of the 677 quantifiable proteins, 11 were associated with cytokine activity (GO:0005125), 12 to growth factor activity (GO:0008083), and 34 to response to hypoxia (GO:0001666). Mapping of all identified proteins to the MEROPS protease database identified 74 different proteases in our dataset (Supplementary Tables S3 and S4).

Top Regulated Proteins

Our analysis identified 34 proteins (4 up- and 30 downregulated) for dry AMD, 33 proteins (30 up- and 3 downregulated) for nAMD, and 142 proteins (84 up- and 58 downregulated) for PDR to be significantly regulated relative to ERM (Fig. 2A). Comparison of these proteins revealed that most were unique to a specific patient group (Fig. 2B). Only ribonuclease (pancreatic; RNAS1) and serine carboxypeptidase (probable; CPVL) were common for dry- and nAMD, as were β-2-microglobulin (B2MG), 14-3-3 protein γ (1433G), retinal dehydrogenase 1 (AL1A1), and protein DJ-1 (PARK7) for nAMD and PDR. Because nAMD and PDR have a common neovascular component, it will be of interest to test whether these proteins are relevant for neovascular processes. The largest overlap was observed for dry AMD and PDR. Proteins detected in the vitreous of both patient groups included HEM2, lithostathine-1-α (REG1A), ICAM1, ribonuclease 4 (RNAS4), scavenger receptor cysteine-rich type 1 protein M130 (F5GZZ9), carboxypeptidase (X6R5C5), actin (cytoplasmic 2; ACTG), and neurosecretory protein VGF (VGF). No protein was found that was differentially regulated in all patient groups.

It is striking that the vast majority (88%) of differentially regulated proteins in dry AMD were downregulated. HEM2, RNAS1, CPVL and cholinesterase (CHLE) were the only four proteins found to be upregulated (Table 1). In contrast, more proteins were up- than downregulated in both nAMD (91%) and PDR (59%). VGFR1, important for the regulation of neovascularization, was the strongest upregulated factor in nAMD, followed by 1433G and AL1A1 (Table 1). The top three upregulated proteins found in PDR were hemoglobin subunit β (HBB), carbonic anhydrase 1 (CAH1), and HEM2 (Table 1).

GSEA and Pathway Mapping

Although identification of specific differentially regulated proteins in individual patient groups is critical for disease characterization and the definition of potential biomarkers, it is of equal importance to describe affected protein and gene networks to approach pathologic mechanisms, even if single members of such networks may not reach significance by the stringent filter criteria set for protein regulation. Thus, potentially relevant gene networks were identified by GSEA,

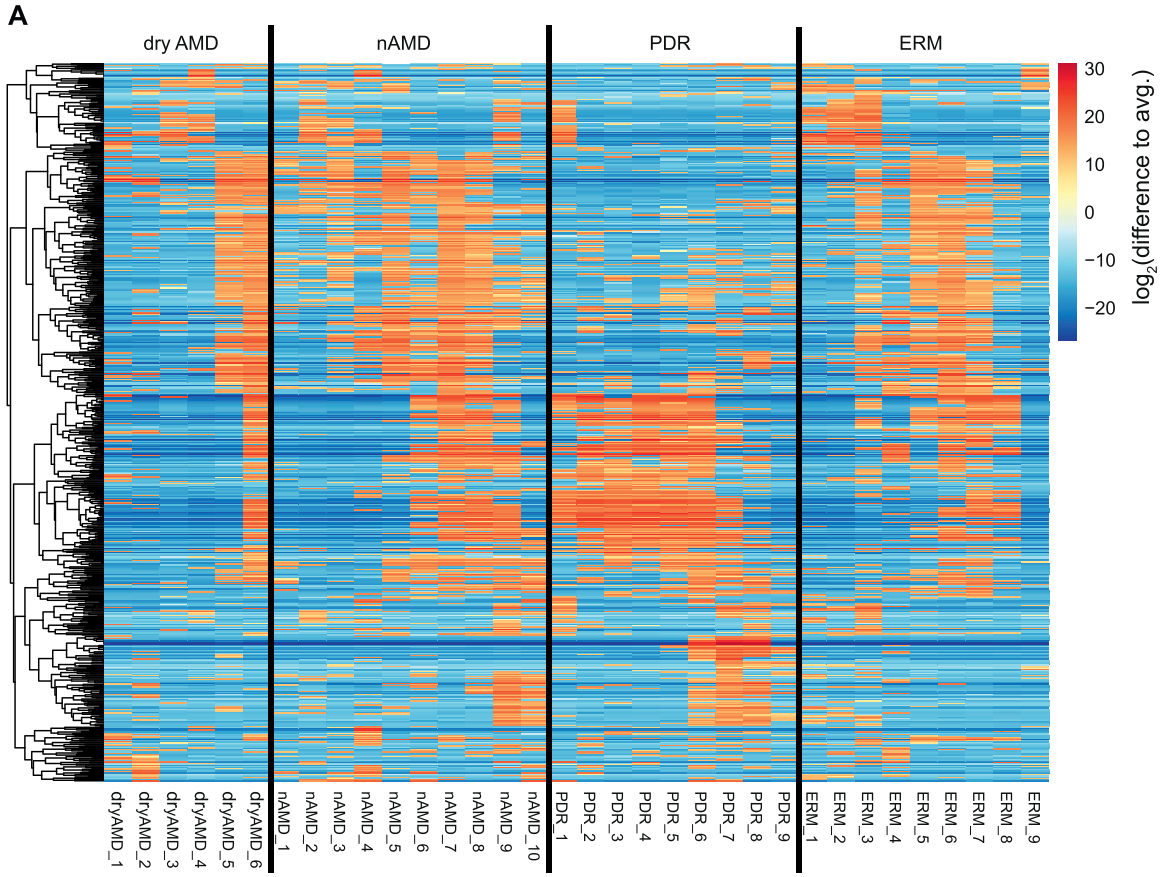

B

dry AMD		
GO-Term	**Description**	**FDR**
GO-BP	response to stress	1.2×10^{-3}
	acute inflammatory response	2.6×10^{-2}
	regulation of immune system process	2.9×10^{-2}
GO-MF	serine-type peptidase activity	1.7×10^{-3}
	cell adhesion molecule binding	1.7×10^{-3}
	integrin binding	3.6×10^{-3}
GO-CC	extracellular region	1.7×10^{-14}
	membrane-bounded vesicle	1.7×10^{-14}
	extracellular exosome	1.7×10^{-14}
nAMD		
GO-Term	**Description**	**FDR**
GO-BP	response to stress	3.3×10^{-6}
	antigen processing and presentation	2.0×10^{-4}
	IFNγ mediated signaling pathway	2.0×10^{-4}
GO-MF	glycoprotein binding	8.9×10^{-3}
	receptor binding	8.9×10^{-3}
	protein binding	8.9×10^{-3}
GO-CC	extracellular region	1.2×10^{-13}
	extracellular exosome	3.9×10^{-13}
	membrane-bounded vesicle	3.7×10^{-12}
PDR		
GO-Term	**Description**	**FDR**
GO-BP	regulation of endopeptidase activity	4.2×10^{-15}
	extracellular matrix organization	1.2×10^{-13}
	regulation of response to wounding	2.1×10^{-12}
GO-MF	endopeptidase inhibitor activity	2.5×10^{-18}
	glycosaminoglycan binding	2.5×10^{-18}
	peptidase regulator activity	8.1×10^{-17}
GO-CC	membrane-bounded vesicle	3.4×10^{-40}
	extracellular space	8.1×10^{-40}
	vesicle	8.7×10^{-40}

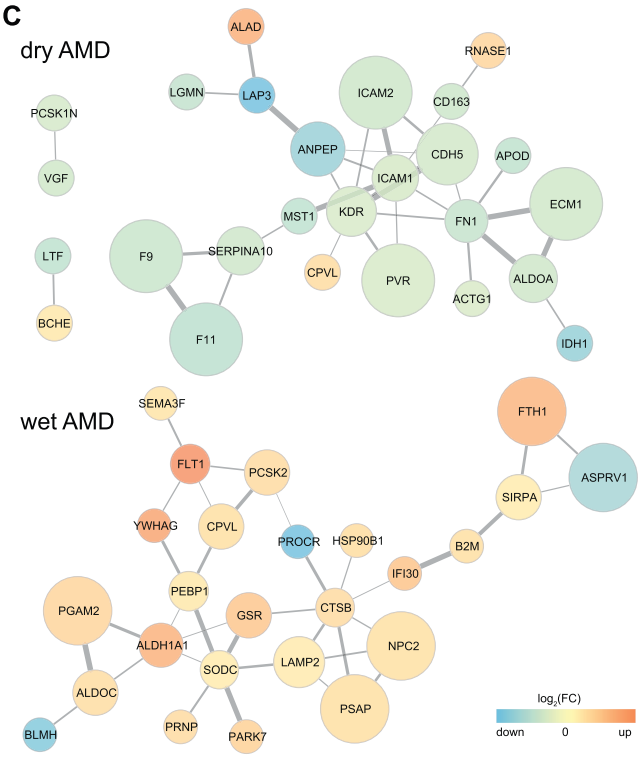

Figure 1. Comparison of the patient groups by heatmap and GO-term analysis. (**A**) Heatmap of normalized relative quantification values with hierarchical Pearson clustering for proteins. Log_2 of quantitative values, centered by subtraction of average values for each protein, is displayed. Higher abundance of a specific protein than average is displayed in *shades of red*, whereas reduced abundance is displayed in *shades of blue*. (**B**) STRING GO-term enrichment of all significantly differentially regulated proteins ($|\log_2(FC)| > 0.58$; $P < 0.05$) in each patient group. The three strongest enriched GO-terms for each of the three parental GO-term categories GO-MF, GO-BP, and GO-CC are listed. (**C**) STRING protein–protein interaction networks of dry AMD and nAMD patient group, based on significantly differentially regulated proteins ($|\log_2(FC)| > 0.58$; $P < 0.05$). Color gradient corresponds to $\log_2(FC)$, node size to clustering coefficient, and edge width to STRING association score.

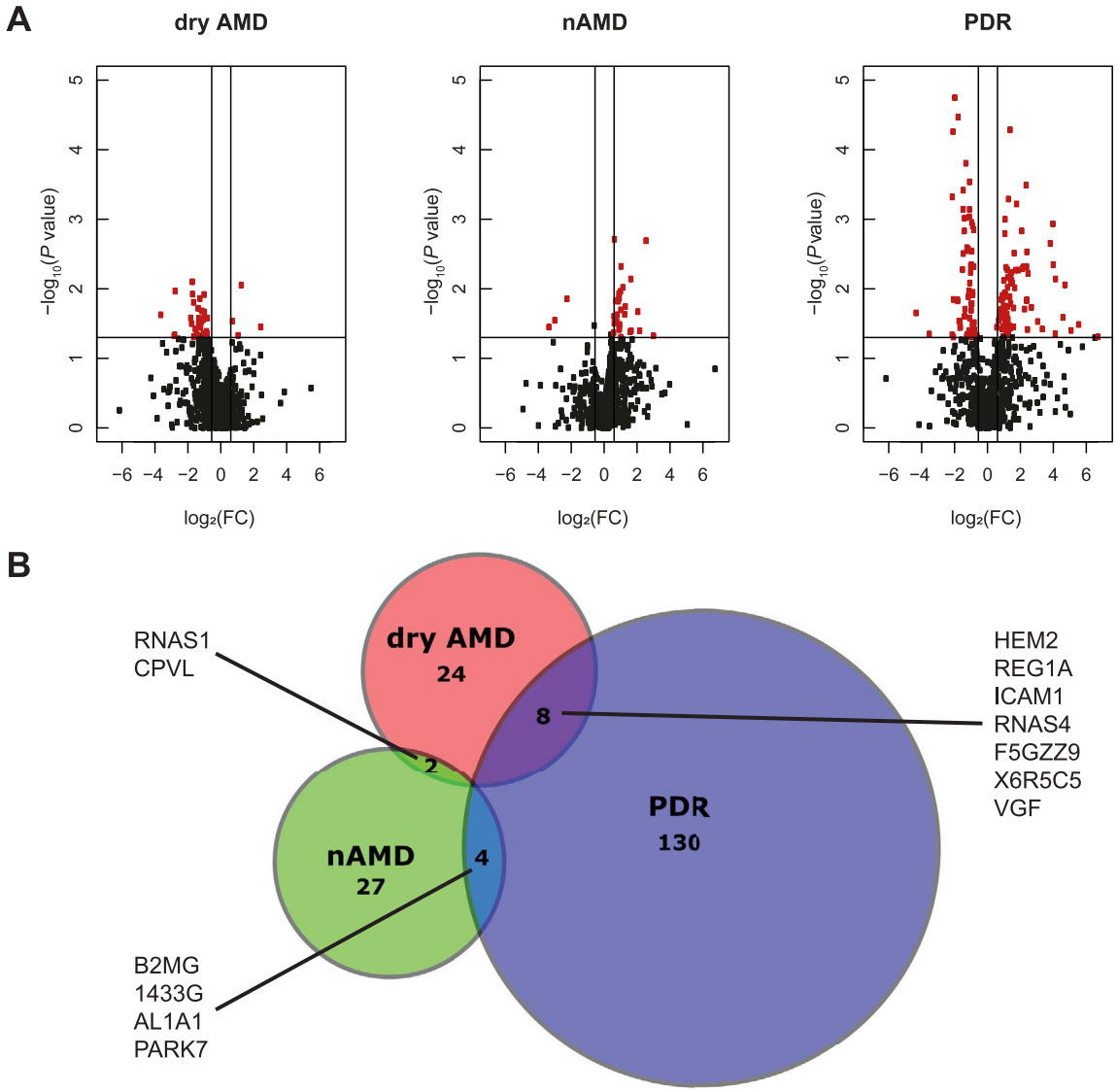

Figure 2. Volcano plots and Venn diagram. (**A**) Volcano plots of all quantified proteins in the respective patient groups relative to the ERM patient group. Significantly differentially regulated proteins ($|\log_2(FC)| > 0.58$; $P < 0.05$) are displayed in *red*. (**B**) Venn diagram identifying the number of significantly differentially regulated proteins, which were common to more than one patient group.

and enriched proteins were mapped to pathway maps (Table 2). Although for dry AMD, no pathway reached the significance threshold, oxidative stress was closest (FDR: 0.261; Table 2) and included glutathione peroxidase 3 (*GPX3*), superoxide dismutase 1 and 3 (*SOD1*, *SOD3*), and catalase (*CAT*) that all showed a trend for upregulation (Supplementary Table S2). For nAMD, the pathway focal adhesion that included *FLT1* and *KDR*, the genes encoding VGFR1 and VGFR2, respectively, had the lowest FDR (0.004) (Table 2). For PDR patients, the pathway complement and coagulation cascade (FDR: 0.024) was among the most enriched pathways (Table 2).

Validation of Proteomics Data by ELISA

Seven proteins identified by proteomics were validated (Fig. 3), and their concentrations determined (Supplementary Table S5) by ELISA. The ELISA data matched the proteomics-based expression pattern of CFAI, CH3L1, HEM2, and SODC in the different patient groups. However, the upregulation of RNAS1 in dry AMD and nAMD and of VGFR1 in nAMD was not reproduced.

Levels of VEGFA, the main regulator of neovascularization, were also determined by ELISA, despite its absence in our proteomics data set. It showed a slight trend toward elevated levels in PDR patients, whereas the other patient groups, including nAMD, did not show any regulation (Fig. 3).

Discussion

AMD is a major cause of blindness or visual impairment in developed countries and the third major cause globally.[45,46] Whereas anti-VEGF therapies can prevent disease progression in nAMD and PDR, no treatment options exist for the highly prevalent dry form of AMD. The identification of biomarkers would not only facilitate diagnosing patients early during disease but also help to understand disease mechanisms and to develop therapies. To use biomarkers in clinics, both the

Table 1. Significantly Upregulated Proteins for Each Patient Group

Protein Name	Gene Name	Description	FC	*P* Value
Dry AMD				
HEM2	*ALAD*	δ-aminolevulinic acid dehydratase	5.5	0.035
RNAS1	*RNASE1*	Ribonuclease pancreatic	2.4	0.009
CPVL	*CPVL*	Probable serine carboxypeptidase CPVL	2.1	0.047
CHLE	*BCHE*	Cholinesterase	1.7	0.029
nAMD				
VGFR1	*FLT1*	Vascular endothelial growth factor receptor 1	8.2	0.047
1433G	*YWHAG*	14-3-3 protein γ	6.0	0.002
AL1A1	*ALDH1A1*	Retinal dehydrogenase 1	4.6	0.040
FRIH	*FTH1*	Ferritin heavy chain	4.3	0.021
GILT	*IFI30*	γ-interferon–inducible lysosomal thiol reductase	3.2	0.040
CH3L1	*CHI3L1*	Chitinase-3-like protein 1	3.2	0.007
GSHR	*GSR*	Isoform 2 of glutathione reductase, mitochondrial	3.1	0.041
PARK7	*PARK7*	Protein DJ-1	2.5	0.018
MASP2	*MASP2*	Mannan-binding lectin serine protease 2	2.4	0.023
PGAM2	*PGAM2*	Phosphoglycerate mutase 2	2.3	0.010
PDR				
HBB	*HBB*	Hemoglobin subunit β	107.8	0.049
CAH1	*CA1*	Carbonic anhydrase 1	47.7	0.033
HEM2	*ALAD*	δ-aminolevulinic acid dehydratase	34.7	0.040
SAA1	*SAA1*	Serum amyloid A-1 protein	26.9	0.009
RINI	*RNH1*	Ribonuclease inhibitor	24.7	0.026
CATA	*CAT*	Catalase	18.0	0.007
CAH2	*CA2*	Carbonic anhydrase 2	17.8	0.044
FIBB	*FGB*	Fibrinogen β chain	16.4	0.004
GUC2A	*GUCA2A*	Guanylin	16.1	0.001
FIBG	*FGG*	Isoform γ-A of fibrinogen γ chain	14.5	0.002

nature of the tissue for analysis and the ease of material sampling must be considered. The VH might be ideal due to its proximity to the retina and its accessibility during vitreoretinal surgery. Thus, several studies used the human VH for MS-based proteomics, but all focused on PDR[21,23,25,47,48] and nAMD.[32,33] Studies concentrating on dry AMD mainly analyzed the composition of drusen,[49,50] the choroid/Bruch membrane complex,[51] or the RPE[52] of post mortem eyes. Here, we

Table 2. Top Five GSEA Positively Enriched Pathways for Each Patient Group

Wiki PW ID	Enriched Pathway	FDR	NES*	Enriched Genes
Dry AMD				
WP408	Oxidative stress	0.261	1.71	*GPX3*; *SOD1*; *SOD3*; *CAT*
WP1533	Vitamin B12 metabolism	0.441	1.34	*ALB*; *HBA1*; *HBB*; *SOD1*
WP176	Folate metabolism	0.485	1.48	*ALB*; *GPX3*; *HBA1*; *HBB*; *SOD1*; *CAT*
WP15	Selenium micronutrient network	0.542	1.16	*ALB*; *GPX3*; *HBA1*; *HBB*; *SOD1*; *CAT*
WP2064	Neural crest differentiation	0.554	1.36	*CDH6*
nAMD				
WP306	Focal adhesion	0.004	1.85	*COL11A1*; *FLNA*; *FLT1*; *KDR*; *ACTB*; *TLN1*; *ACTG1*
WP51	Regulation of actin cytoskeleton	0.007	1.80	*CFL1*; *MSN; PFN1*; *ACTB*; *ACTG1*; *EZR*
WP289	Myometrial relaxation and contraction pathways	0.012	1.75	*GUCA2A*; *ACTB*; *ACTC1*; *ACTG1*; *YWHAV*; *YWHAG*; *YWHAZ*; *CALM1*; *GSTO1*
WP2884	NRF2 pathway	0.049	1.65	*FTH1*; *FLT*; *GSR*; *GSTP1*; *HSP90AA1*; *PGD*; *SERPINA1*; *CBR1*
WP534	Glycolysis and gluconeogenesis	0.081	1.58	*ENO1*; *FBP1*; *ALDOA*; *ALDOC*; *GAPDH*; *GPI*; *LDHA*; *MDH1*; *PGAM2*; *PGK1*; *PKM*; *TPI1*
PDR				
WP15	Selenium micronutrient network	0.016	1.83	*CRP*; *GSR*; *HBA1*; *HBB*; *APOB*; *SAA1*; *PRDX2*; *CAT*
WP558	Complement coagulation cascades	0.024	1.78	*MASP2*; *CPB2*; *CFD*; *F2*; *F9*; *F12*; *F13B*; *FGB*; *SERPIND1*; *CFI*; *KLKB1*; *KNG1*; *SERPINC1*; *SERPINA5*; *PLG*; *SERPINF2*; *PROS1*; *CFB*; *SERPING1*; *C1QB*; *C1R*; *C1S*; *C2*; *C3*; *C4B*; *C6*; *C7*; *C8G*; *C9*; *VWF*
WP2884	NRF2 pathway	0.056	1.66	*FTH1*; *FTL*; *GSR*; *PGD*; *BLVRB*; *PRDX6*
WP176	Folate metabolism	0.060	1.69	*CRP*; *HBA1*; *HBB*; *APOB*; *SAA1*; *CAT*
WP1533	Vitamin B12 metabolism	0.070	1.66	*CRP*; *HBA1*; *HBB*; *APOB*; *SAA1*

* Normalized enrichment score.

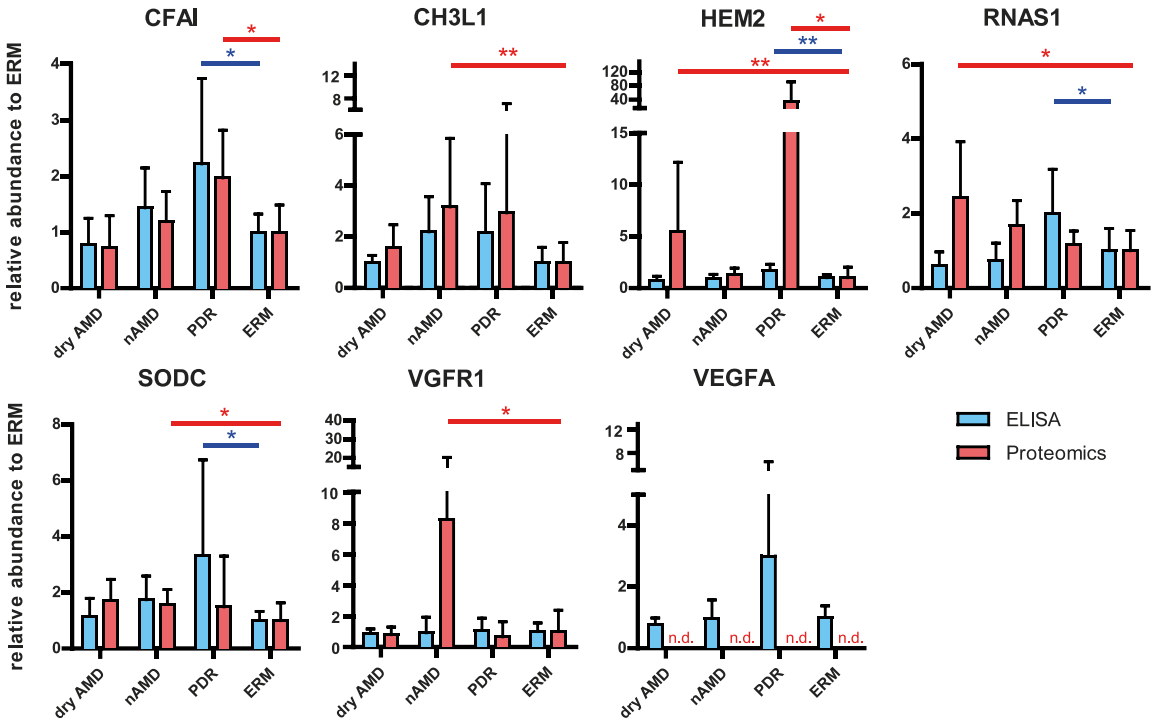

Figure 3. Validation of proteomics data by ELISA. Comparison of protein abundance measured by ELISA (*blue*) to LC-MS/MS based proteomics (*red*) measurements. Protein levels were expressed relative to the ERM patient group. Shown are means ± SD. $^{*}P < 0.05$; $^{**}P < 0.01$.

directly compared the VH proteome of dry AMD, nAMD, PDR, and ERM patients.

We found that 195 of the 677 proteins identified in our patient groups were significantly regulated (Fig. 2B). Of the 34 proteins identified in dry AMD, only HEM2, RNAS1, CPVL, and CHLE were upregulated. The only protein upregulated solely in dry AMD was CHLE. It is a ubiquitously expressed protein that regulates cell proliferation in embryonic tissues and the onset of differentiation during early neuronal development.[53] CHLE has neuroprotective potential and is used to prevent nerve agent toxicity[54] and, in a modified form, as cocaine addiction therapeutic.[55] HEM2 was upregulated also in PDR and is involved in catalyzing the condensation of δ-aminolevulinic acid (ALA) to porphobilinogen.[56] This activity may reduce oxidative stress as ALA is a potential source of reactive oxygen species due to autoxidation.[57] CPVL, an enzyme potentially involved in antigen processing,[58] was upregulated in dry AMD and nAMD but downregulated in PDR. Interestingly, a single nucleotide polymorphism (SNP) in a haplotype block that included *CPVL* was associated with diabetic retinopathy in Chinese patients.[59] Similar to CPVL, RNAS1, which is secreted and responsible for the degradation of extracellular RNA,[60–62] was upregulated in dry AMD and nAMD.

Choroidal or retinal neovascularization are central hallmarks of nAMD and PDR, respectively.[63] The most prominent and therapeutically relevant factor for neovascularization is VEGF, overexpressed either from the RPE (nAMD) or pericytes (PDR).[64,65] However, our own and most of the published VH discovery proteomics studies performed by MS did not detect VEGF as differentially regulated factor.[23–25,33,47] The generally low levels of VEGF and only minor concentration changes in focal areas may explain the lack of detection by global methods such as LC-MS/MS.[47] ELISA, however, detected VEGF and showed increased (nonsignificant) levels in PDR but not nAMD (Fig. 3). In contrast, VGFR1 (8.2×, $P = 0.047$; Table 1) and VGFR2 (109×, nonsignificant), the two receptors for VEGF, were upregulated in nAMD, but only VGFR2 (2.6×, nonsignificant) was found increased also in PDR (Supplementary Table S2). The varying regulation of these factors might be explained by the treatment of nAMD and PDR patients with anti-VEGF or laser photocoagulation therapy, respectively.

As oxidative stress due to cigarette smoke,[66] exposure to sunlight,[67] and other environmental factors is likely contributing to AMD development, it may be of significance that the NRF2 pathway that regulates a protective antioxidant response[68] was found enriched in nAMD and PDR by GSEA analysis (Table 2). Oxidative stress may also be important for dry AMD[69] because *GPX3*, *SOD1*, *SOD3*, and *CAT* involved in the regulation of reactive oxygen species and part of the oxidative stress pathway were upregulated (Table 2; Supplementary Table S2), even though enrichment was weak (FDR: 0.261).

For nAMD, the focal adhesion pathway was strongly enriched (0.004 FDR; Table 2). This may correlate to the reported high incidence of focal vitreomacular adhesions at the site of choroidal neovascularization in nAMD patients.[70] Further, the enrichment of the pathway for glycolysis and gluconeogenesis (FDR: 0.081) potentially indicates a metabolic shift to aerobic glycolysis. Increased levels of lactate dehydrogenase (LDHA; Table 2; Supplementary Table S2) could be a consequence of the Warburg effect as it has been reported for nAMD patients.[71] Increased conversion of pyruvate to lactate as it occurs during glycolysis is also suggested by data showing higher urinary lactate/pyruvate ratios in nAMD patients.[72]

Low level complement activation is part of the immune tolerance in the immune privileged eye.[73] Dysregulation of the complement system has been linked to AMD,[74] and genome-wide association studies have identified several SNPs in genes of the complement system to be risk factors for the development of AMD[75] and PDR.[76] Similarly to our data showing a strong enrichment (FDR: 0.024) of the pathway complement and coagulation cascade in PDR patients with significant upregulation of 11 of 27 mapped proteins, an enrichment of complement cascade components in the VH of

PDR patients has been reported.[47] Conversely in dry AMD patients, complement factor H (CFAH) and complement factor H-related protein 1 (FHR1)—the only components of the alternative pathway able to suppress complement activation on extracellular matrix[75]—showed reduced levels (Supplementary Table S2).

As expected for a mostly acellular structure such as the VH, GO-CC was strongly enriched for extracellular terms including extracellular region in dry AMD and nAMD and extracellular space and others in PDR (Fig. 1B). Nevertheless, total GO-CC categorization revealed that a majority (56%) of all identified proteins were membrane associated or intracellular. Because 7 (APOE; MYH9; PHLD; Q5H9A7; TIMP2; DAG1; and ERAP1) of the 74 identified human proteases belonged to a disintegrin and metalloprotease (ADAM) family, increased ectodomain shedding may explain this observation, as has been suggested for PDR patients.[47]

Conclusions

The direct comparison of the VH proteome of dry AMD, nAMD, and PDR to ERM patients identified different clusters of upregulated proteins for each patient group and showed characteristic enrichment of specific pathways, such as oxidative stress for dry AMD, focal adhesion for nAMD, and complement and coagulation cascade for PDR. We identified CHLE to be specifically upregulated in dry AMD and RNAS1 together with CPVL to be upregulated in both forms of AMD. The relevance of these factors needs to be investigated in additional studies with larger patient cohorts.

Acknowledgments

The authors thank the surgical team and the nurses of the ophthalmology department of the University Hospital of Zurich for sample collection; Sarah Steinmann and Elena Lüssi for coordination of patients and sample aliquoting; and all the volunteers for cooperation in this study.

Supported by Novartis Pharma Switzerland Research Agreement W-15/622 and Swiss National Science Foundation Grants 31003A_149311 and 31003A_173008.

Disclosure: **C. Schori**, None; **C. Trachsel**, None; **J. Grossmann**, None; **I. Zygoula**, None; **D. Barthelmes**, None; **C. Grimm**, None

References

1. Klein R, Klein BE, Linton KL. Prevalence of age-related maculopathy. The Beaver Dam Eye Study. *Ophthalmology*. 1992;99:933–943.
2. Mitchell P, Smith W, Attebo K, Wang JJ. Prevalence of age-related maculopathy in Australia. The Blue Mountains Eye Study. *Ophthalmology*. 1995;102:1450–1460.
3. Vingerling JR, Dielemans I, Hofman A, et al. The prevalence of age-related maculopathy in the Rotterdam Study. *Ophthalmology*. 1995;102:205–210.
4. Bird AC. Choroidal neovascularisation in age-related macular disease. *Br J Ophthalmol*. 1993;77:614–615.
5. Ferris FL, Fine SL, Hyman L. Age-related macular degeneration and blindness due to neovascular maculopathy. *Arch Ophthalmol (Chicago, Ill 1960)*. 1984;102:1640–1642.
6. Leibowitz HM, Krueger DE, Maunder LR, et al. The Framingham Eye Study monograph: an ophthalmological and epidemiological study of cataract, glaucoma, diabetic retinopathy, macular degeneration, and visual acuity in a general population of 2631 adults, 1973-1975. *Surv Ophthalmol*. 1980;24:335–610.
7. Argon laser photocoagulation for senile macular degeneration. Results of a randomized clinical trial. *Arch Ophthalmol (Chicago, Ill 1960)*. 1982;100:912–918.
8. Group MPS. Krypton laser photocoagulation for neovascular lesions of age-related macular degeneration. Results of a randomized clinical trial. Macular Photocoagulation Study Group. *Arch Ophthalmol (Chicago, Ill 1960)*. 1990;108:816–824.
9. Macular Photocoagulation Study Group. Laser photocoagulation of subfoveal neovascular lesions of age-related macular degeneration: updated findings from two clinical trials. *Arch Ophthalmol (Chicago, Ill 1960)*. 1993;111:1200–1209.
10. Edwards AO, Ritter R, Abel KJ, Manning A, Panhuysen C, Farrer LA. Complement factor H polymorphism and age-related macular degeneration. *Science*. 2005;308:421–424.
11. Haines JL, Hauser MA, Schmidt S, et al. Complement factor H variant increases the risk of age-related macular degeneration. *Science*. 2005;308:419–421.
12. Khan JC, Thurlby DA, Shahid H, et al. Smoking and age related macular degeneration: the number of pack years of cigarette smoking is a major determinant of risk for both geographic atrophy and choroidal neovascularisation. *Br J Ophthalmol*. 2006;90:75–80.
13. Klein BE, Klein R, Lee KE, Jensen SC. Measures of obesity and age-related eye diseases. *Ophthalmic Epidemiol*. 2001;8:251–262.
14. Klein RJ, Zeiss C, Chew EY, et al. Complement factor H polymorphism in age-related macular degeneration. *Science*. 2005;308:385–389.
15. Seddon JM, Cote J, Rosner B. Progression of age-related macular degeneration: association with dietary fat, transunsaturated fat, nuts, and fish intake. *Arch Ophthalmol*. 2003;121:1728–1737.
16. Grunwald JE, Metelitsina TI, Dupont JC, Ying G-S, Maguire MG. Reduced foveolar choroidal blood flow in eyes with increasing AMD severity. *Invest Ophthalmol Vis Sci*. 2005;46:1033–1038.
17. Brown DM, Kaiser PK, Michels M, et al. Ranibizumab versus verteporfin for neovascular age-related macular degeneration. *N Engl J Med*. 2006;355:1432–1444.
18. Rosenfeld PJ, Brown DM, Heier JS, et al. Ranibizumab for neovascular age-related macular degeneration. *N Engl J Med*. 2006;355:1419–1431.
19. Heier JS, Antoszyk AN, Pavan PR, et al. Ranibizumab for treatment of neovascular age-related macular degeneration: a phase I/II multicenter, controlled, multidose study. *Ophthalmology*. 2006;113:633.e1–e4.
20. Martin DF, Maguire MG, Ying GS, Grunwald JE, Fine SL, Jaffe GJ; for the CATT Research Group. Ranibizumab and bevacizumab for neovascular age-related macular degeneration. *N Engl J Med*. 2011;364:1897–1908.
21. Shitama T, Hayashi H, Noge S, et al. Proteome profiling of vitreoretinal diseases by cluster analysis. *Proteomics Clin Appl*. 2008;2:1265–1280.
22. Wu CW, Sauter JL, Johnson PK, Chen C-D, Olsen TW. Identification and localization of major soluble vitreous proteins in human ocular tissue. *Am J Ophthalmol*. 2004;137:655–661.
23. Gao B-BB, Chen X, Timothy N, Aiello LP, Feener EP. Characterization of the vitreous proteome in diabetes without diabetic retinopathy and diabetes with proliferative diabetic retinopathy. *J Proteome Res*. 2008;7:2516–2525.
24. Kim T, Kim SJ, Kim K, et al. Profiling of vitreous proteomes from proliferative diabetic retinopathy and nondiabetic patients. *Proteomics*. 2007;7:4203–4215.
25. Wang H, Feng L, Hu J, Xie C, Wang F. Differentiating vitreous proteomes in proliferative diabetic retinopathy using high-

performance liquid chromatography coupled to tandem mass spectrometry. *Exp Eye Res*. 2013;108:110–119.

26. Murthy KR, Goel R, Subbannayya Y, et al. Proteomic analysis of human vitreous humor. *Clin Proteomics*. 2014;11:29.
27. Aretz S, Krohne TU, Kammerer K, et al. In-depth mass spectrometric mapping of the human vitreous proteome. *Proteome Sci*. 2013;11:22.
28. Angi M, Kalirai H, Coupland SE, Damato BE, Semeraro F, Romano MR. Proteomic analyses of the vitreous humour. *Mediators Inflamm*. 2012;2012:148039.
29. Bennett KL, Funk M, Tschernutter M, et al. Proteomic analysis of human cataract aqueous humour: comparison of one-dimensional gel LCMS with two-dimensional LCMS of unlabelled and iTRAQ®-labelled specimens. *J Proteomics*. 2011;74:151–166.
30. Pollreisz A, Funk M, Breitwieser FP, et al. Quantitative proteomics of aqueous and vitreous fluid from patients with idiopathic epiretinal membranes. *Exp Eye Res*. 2013;108:48–58.
31. Yu J, Peng R, Chen H, Cui C, Ba J. Elucidation of the pathogenic mechanism of rhegmatogenous retinal detachment with proliferative vitreoretinopathy by proteomic analysis. *Invest Ophthalmol Vis Sci*. 2012;53:8146–8153.
32. Nobl M, Reich M, Dacheva I, et al. Proteomics of vitreous in neovascular age-related macular degeneration. *Exp Eye Res*. 2016;146:107–117.
33. Koss MJ, Hoffmann J, Nguyen N, et al. Proteomics of vitreous humor of patients with exudative age-related macular degeneration. *PLoS One*. 2014;9:e96895.
34. Lobo A, Lightman S. Vitreous aspiration needle tap in the diagnosis of intraocular inflammation. *Ophthalmology*. 2003;110:595–599.
35. Wiśniewski JR, Zougman A, Nagaraj N, Mann M. Universal sample preparation method for proteome analysis. *Nat Methods*. 2009;6:359–362.
36. Käll L, Storey JD, MacCoss MJ, Noble WS. Assigning significance to peptides identified by tandem mass spectrometry using decoy databases. *J Proteome Res*. 2008;7:29–34.
37. Szklarczyk D, Franceschini A, Wyder S, et al. STRING v10: protein-protein interaction networks, integrated over the tree of life. *Nucleic Acids Res*. 2015;43:D447–D452.
38. Rawlings ND, Barrett AJ, Finn R. Twenty years of the MEROPS database of proteolytic enzymes, their substrates and inhibitors. *Nucleic Acids Res*. 2016;44:D343–D350.
39. R Core Team. *R: A Language and Environment for Statistical Computing*. Vienna, Austria; 2017.
40. Hulsen T, de Vlieg J, Alkema W. BioVenn: a web application for the comparison and visualization of biological lists using area-proportional Venn diagrams. *BMC Genomics*. 2008;9:488.
41. Wang J, Vasaikar S, Shi Z, Greer M, Zhang B. WebGestalt 2017: a more comprehensive, powerful, flexible and interactive gene set enrichment analysis toolkit. *Nucleic Acids Res*. 2017;45:W130–W137.
42. Kutmon M, Riutta A, Nunes N, et al. WikiPathways: capturing the full diversity of pathway knowledge. *Nucleic Acids Res*. 2016;44:D488–D494.
43. Subramanian A, Tamayo P, Mootha VK, et al. Gene set enrichment analysis: a knowledge-based approach for interpreting genome-wide expression profiles. *Proc Natl Acad Sci U S A*. 2005;102:15545–15550.
44. Vizcaíno JA, Csordas A, Del-Toro N, et al. 2016 update of the PRIDE database and its related tools. *Nucleic Acids Res*. 2016;44:D447–D456.
45. Pascolini D, Mariotti SP, Pokharel GP, et al. 2002 global update of available data on visual impairment: a compilation of population-based prevalence studies. *Ophthalmic Epidemiol*. 2004;11:67–115.
46. Mitchell J, Bradley C. Quality of life in age-related macular degeneration: a review of the literature. *Health Qual Life Outcomes*. 2006;4:97.
47. Loukovaara S, Nurkkala H, Tamene F, et al. Quantitative proteomics analysis of vitreous humor from diabetic retinopathy patients. *J Proteome Res*. 2015;14:5131–5143.
48. Yamane K, Minamoto A, Yamashita H, et al. Proteome analysis of human vitreous proteins. *Mol Cell Proteomics*. 2003;2:1177–1187.
49. Crabb JW, Miyagi M, Gu X, et al. Drusen proteome analysis: an approach to the etiology of age-related macular degeneration. *Proc Natl Acad Sci U S A*. 2002;99:14682–14687.
50. Umeda S, Suzuki MT, Okamoto H, et al. Molecular composition of drusen and possible involvement of anti-retinal autoimmunity in two different forms of macular degeneration in cynomolgus monkey (*Macaca fascicularis*). *FASEB J*. 2005;19:1683–1685.
51. Yuan X, Gu X, Crabb JS, et al. Quantitative proteomics: comparison of the macular Bruch membrane/choroid complex from age-related macular degeneration and normal eyes. *Mol Cell Proteomics*. 2010;9:1031–1046.
52. Nordgaard CL, Karunadharma PP, Feng X, Olsen TW, Ferrington DA. Mitochondrial proteomics of the retinal pigment epithelium at progressive stages of age-related macular degeneration. *Invest Ophthalmol Vis Sci*. 2008;49:2848–2855.
53. Mack A, Robitzki A. The key role of butyrylcholinesterase during neurogenesis and neural disorders: an antisense-5′butyrylcholinesterase-DNA study. *Prog Neurobiol*. 2000;60:607–628.
54. Lockridge O. Review of human butyrylcholinesterase structure, function, genetic variants, history of use in the clinic, and potential therapeutic uses. *Pharmacol Ther*. 2015;148:34–46.
55. Murthy V, Gao Y, Geng L, LeBrasseur N, White T, Brimijoin S. Preclinical studies on neurobehavioral and neuromuscular effects of cocaine hydrolase gene therapy in mice. *J Mol Neurosci*. 2014;53:409–416.
56. Jaffe EK, Martins J, Li J, Kervinen J, Dunbrack RL. The molecular mechanism of lead inhibition of human porphobilinogen synthase. *J Biol Chem*. 2001;276:1531–1537.
57. Princ FG, Maxit AG, Cardalda C, Batlle A, Juknat AA. In vivo protection by melatonin against delta-aminolevulinic acid-induced oxidative damage and its antioxidant effect on the activity of haem enzymes. *J Pineal Res*. 1998;24:1–8.
58. Harris J, Schwinn N, Mahoney JA, et al. A vitellogenic-like carboxypeptidase expressed by human macrophages is localized in endoplasmic reticulum and membrane ruffles. *Int J Exp Pathol*. 2006;87:29–39.
59. Hu C, Zhang R, Yu W, et al. CPVL/CHN2 genetic variant is associated with diabetic retinopathy in Chinese type 2 diabetic patients. *Diabetes*. 2011;60:3085–3089.
60. Sorrentino S. Human extracellular ribonucleases: multiplicity, molecular diversity and catalytic properties of the major RNase types. *Cell Mol Life Sci*. 1998;54:785–794.
61. Fischer S, Nishio M, Dadkhahi S, et al. Expression and localisation of vascular ribonucleases in endothelial cells. *Thromb Haemost*. 2011;105:345–355.
62. Gansler J, Preissner KT, Fischer S. Influence of proinflammatory stimuli on the expression of vascular ribonuclease 1 in endothelial cells. *FASEB J*. 2014;28:752–760.
63. Kvanta A. Ocular angiogenesis: the role of growth factors. *Acta Ophthalmol Scand*. 2006;84:282–288.
64. Witmer A. Vascular endothelial growth factors and angiogenesis in eye disease. *Prog Retin Eye Res*. 2003;22:1–29.

Investigative Ophthalmology & Visual Science

65. Sene A, Chin-Yee D, Apte R. Seeing through VEGF: innate and adaptive immunity in pathologic angiogenesis in the eye. *Trends Mol Med*. 2015;1:43–51.
66. Seddon JM, George S, Rosner B. Cigarette smoking, fish consumption, omega-3 fatty acid intake, and associations with age-related macular degeneration: the US Twin Study of Age-Related Macular Degeneration. *Arch Ophthalmol (Chicago, Ill 1960)*. 2006;124:995–1001.
67. Schick T, Ersoy L, Lechanteur YTE, et al. History of sunlight exposure is a risk factor for age-related macular degeneration. *Retina*. 2016;36:787–790.
68. Batliwala S, Xavier C, Liu Y, Wu H, Pang I. Involvement of Nrf2 in ocular diseases. *Oxid Med Cell Longev*. 2017;2017:1703810.
69. Datta S, Cano M, Ebrahimi K, Wang L, Handa JT. The impact of oxidative stress and inflammation on RPE degeneration in non-neovascular AMD. *Prog Retin Eye Res*. 2017;60:201–218.
70. Mojana F, Cheng L, Bartsch DG, et al. The role of abnormal vitreomacular adhesion in age-related macular degeneration: spectral optical coherence tomography and surgical results. *Am J Ophthalmol*. 2008;146:218–227.
71. Vallée A, Lecarpentier Y, Guillevin R, Vallée JN. Aerobic glycolysis hypothesis through WNT/Beta-catenin pathway in exudative age-related macular degeneration. *J Mol Neurosci*. 2017;62:368–379.
72. Yokosako K, Mimura T, Funatsu H, et al. Glycolysis in patients with age-related macular degeneration. *Open Ophthalmol J*. 2014;8:39–47.
73. Niederkorn JY, Kaplan HJ. Rationale for immune response and the eye. *Chem Immunol Allergy*. 2007;92:1–3.
74. Anderson DH, Radeke MJ, Gallo NB, et al. The pivotal role of the complement system in aging and age-related macular degeneration: hypothesis re-visited. *Prog Retin Eye Res*. 2010; 29:95–112.
75. Clark SJ, Bishop PN. The eye as a complement dysregulation hotspot. *Semin Immunopathol*. 2017;84:65–76.
76. Jha P, Bora PS, Bora NS. The role of complement system in ocular diseases including uveitis and macular degeneration. *Mol Immunol*. 2007;44:3901–3908.

Investigative Ophthalmology & Visual Science